doi:10.1017/S1431927621010035
Microsc. Microanal. 27 (Suppl 1), 2021
© Microscopy Society of America 2021

Crystalline Phase Control in $Sc_XAl_{X-1}N$ Grown by Molecular Beam Epitaxy

Andrew Lang, Matthew Hardy, Brian Downey, Eric Jin, Neeraj Nepal, D. Scott Katzer, David Meyer and Rhonda Stroud

U.S. Naval Research Laboratory, United States

The unique properties of $Sc_XAl_{X-1}N$ thin films have attracted significant attention based on the potential for improved performance in next-generation solid-state and acoustoelectric RF devices [1]. $Sc_XAl_{X-1}N$ is formed by adding cubic ScN, Fm-3m, to wurtzite AlN, $P6_3mc$, which both softens the bonding and increases the polarization compared to AlN. High Sc compositions, x = 0.43, exhibit a 5x increase in piezoresponse compared to pure AlN making $Sc_XAl_{X-1}N$ an extremely attractive candidate for future broadband filters for 5G frequencies [2]. Recently, sputtered polycrystalline $Sc_XAl_{X-1}N$ films with x > 0.27 have been shown to exhibit ferroelectricity, providing evidence that $Sc_XAl_{X-1}N$ may be the first experimentally demonstrated nitride ferroelectric [3]. Controlling the phase of epitaxially grown $Sc_XAl_{X-1}N$ is very challenging due to the interplay of misfit strain, Sc incorporation during growth, and the effect these factors have on the hexagonal/cubic phase boundary in the $Sc_XAl_{X-1}N$ alloy phase diagram. Transmission electron microscopy analysis is ideally suited to examine the local structural morphologic, defect, and phase/growth relationships resulting from film epitaxial growth.

In this study, we examine the structure of $Sc_XAl_{X-1}N$ films grown on SiC via molecular beam epitaxy (MBE) with *in situ* reflection high-energy electron diffraction (RHEED) and post-growth cross-sectional aberration-corrected scanning transmission electron microscopy (STEM). Experimental HAADF and spectroscopy measurements were acquired with an aberration-correctedNionUltraSTEM 200X operated at 200 kV, with a convergence angle of 27 mrad. The RHEED patterns showed that growth of $Sc_XAl_{X-1}N$, with x = 0.4, starts with a significant cubic character, and later transitions to the desired wurtzite phase. STEM analysis, shown in Figure 1a, reveals the complex microstructural growth. Low magnification imaging shows that the initial the film growth proceeds with narrow columnar domains that coarsen into larger domains with several inclined threading dislocations, consistent with strain relief. Closer examination with high resolution high-angle annular dark-field imaging, figure 1b, confirms the RHEED observations. Cubic inclusions are found among the initial columnar growth features, and occasional few-nm cubic grains are also found throughout the coarser grained regions of film. Energy-dispersive x-ray spectroscopy (EDS) mapping confirms the expected x = 0.4 composition of the film, with no clear difference between cubic and hexagonal ScAlN grain compositions. Unlike EDS, electron energy-loss spectroscopy (EELS), shown in Figure 2, reveals a subtle difference between the cubic and hexagonal phases. Due to the convolution of the Sc L- and N K-edges direct interpretation of the edge feature observed at 401eV is challenging, but the cubic phase shows a clear shift of 0.6eV to higher energy. This difference is likely due to the different bond distributions in the cubic and hexagonal lattices, and may serve as a fingerprint to spectroscopically distinguish these phases. Recent modification of the growth parameters has resulted in higher phase purity and a reduced density of inclined threading dislocations. Future work will seek to confirm the predicted ferroelectric behavior of hexagonal films with multiple methods, including high-resolution STEM imaging.

https://doi.org/10.1017/S1431927621010035 Published online by Cambridge University Press

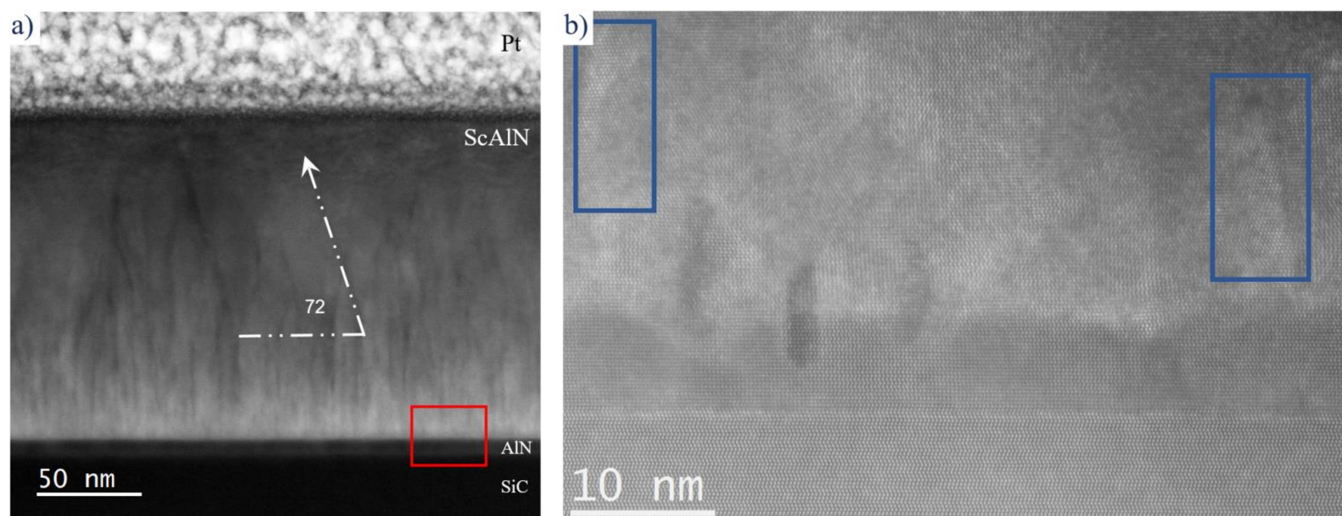

Figure 1. Figure 1. STEM imaging of epitaxially grown Sc0.4Al0.6N film. a) low magnification HAADF image showing the complex microstructure present in the grown film. Note the columnar domains at the bottom of the film which transition to larger domains with inclined threading dislocations highlighted in the film. b) is from the area shown in red in a), and shows a high resolution HAADF image near the AlN/Sc0.4Al0.6N interface. Cubic Sc0.4Al0.6N inclusions are shown in the blue boxes.

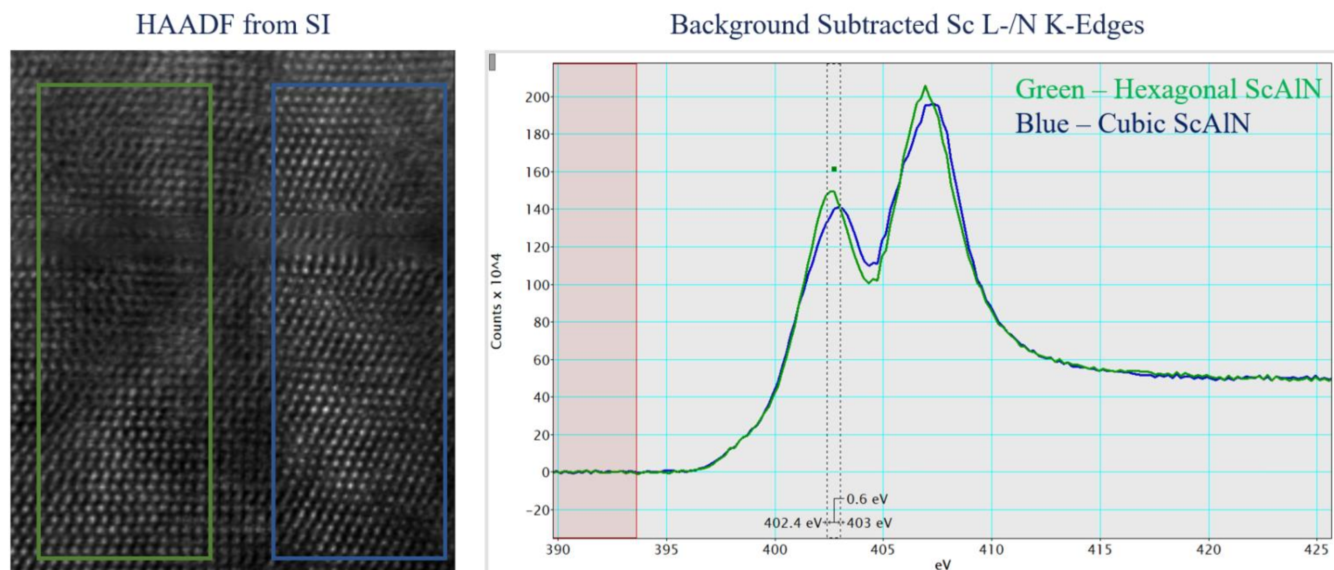

Figure 2. Figure 2. HAADF imaging and EELS analysis of the cubic and hexagonal Sc0.4Al0.6N grains. Left, shows the simultaneously acquired HAADF image from the EELS SI clearly showing the two different phases. Right, extracted equal area EELS maps from the same SI shown on the left of the two different phases. The convoluted Sc L-/N K-edges shown here are background subtracted and overlaid, no other process was done to the data.

References

[1] M. Hardy, E. Jin, N. Nepal, D. S. Katzter*et al* 2020 Appl. Phys. Express 13 065509
[2] M. Akiyama, K. Kano, A. Teshigahara, Appl. Phys. Lett., 95 (2009) 162107
[3] S. Fichtner, N. Wolff, N. Lofink, *et al* Appl. Phys., 125 (2019) 1141

https://doi.org/10.1017/S1431927621010035 Published online by Cambridge University Press